BNL-61588
CONF-9511128--2

PROBABILISTIC WIND/TORNADO/MISSILE ANALYSES FOR HAZARD AND FRAGILITY EVALUATIONS*

by

Young J. Park and Morris Reich
Brookhaven National Laboratory
P.O. Box 5000
Upton, NY 11973

ABSTRACT

Detailed analysis procedures and examples are presented for the probabilistic evaluation of hazard and fragility against high wind, tornado, and tornado-generated missiles. In the tornado hazard analysis, existing risk models are modified to incorporate various uncertainties including modeling errors. A significant feature of this paper is the detailed description of the Monte-Carlo simulation analyses of tornado-generated missiles. A simulation procedure, which includes the wind field modeling, missile injection, solution of flight equations, and missile impact analysis, is described with application examples.

INTRODUCTION

As part of the external event PRA of the High Flux Beam Reactor (HFBR), hazard and fragility analyses were performed against a combined tornado and high wind hazard (Ref. [1]). This paper summarizes the methodology development and application examples in the following areas:

- Tornado hazard analysis;
- Combined tornado/straight wind hazard evaluation;
- Fragility evaluation of structures against wind pressures;
- Analysis of tornado-borne missiles; and
- Fragility evaluation of equipment.

Although the presented hazard and fragility analyses generally follow the methodologies available in open literatures (e.g., Refs. [2], [3] and [4]), some new developments are also introduced in the areas related to the tornado hazard analysis and the tornado-borne missile analysis, including a comprehensive Monte-Carlo simulation scheme for the tornado-borne missile evaluation.

TORNADO HAZARD ANALYSIS

The tornado hazard model described in Reinhold and Ellingwood (1982), that was originally proposed by Garson et al. (1975), is used after a few modifications.

The model is an outgrowth of the earlier models by Fujita (Ref. [9]) and McDonald (Ref. [10]), and is formulated by 6x6 matrices corresponding to Fujita's scale of F0 to F5 intensities. Because of this format, various sources of uncertainties can be systematically combined.

All the variables in the model are discretized according to the FPP scale as given in Table 1 and the associated median wind speed V_i, as

$$\{P_t(V_i)\} = \{P_{ps}(V_i)\} + \{P_{ll}(V_i)\}, \quad i = F0 \text{ to } F5 \qquad (1)$$

in which, $P_t(V_i)$ is the total tornado strike probability associated with the wind speed V_i; $P_{ps}(V_i)$ is the point-strike probability; and $P_{ll}(V_i)$ is the strike probability due to life-line term, reflecting on the increase due to the size of a structure. P_{ps} and P_{ll} are expressed as,

*This work was performed under the auspices of the U.S. Department of Energy.

Table 1 Fujita-Pearson (FPP) Classifications

Fujita Scale	Maximum Wind Speed					
	F0	F1	F2	F3	F4	F5
Range, mph Median, mph	40-72 56.0	73-112 92.5	113-157 135.0	158-206 182.0	207-260 233.5	261-318 289.5
Pearson Path Length Scale	Path Length					
	P0	P1	P2	P3	P4	P5
Range, mi Median, mi	0.3-0.9 0.6	1.0-3.2 2.05	3.2-9.9 6.55	10.0-31.5 20.75	31.6-99 65.3	100-316 208
Pearson Path Width Scale	Path Width					
	P0	P1	P2	P3	P4	P5
Range, yds Median, yds	6-17 11.5	18-55 36.5	56-175 115.5	176-556 366	557-1759 1158	1760-4963 3361.5

$$\{P_{ps}(V_i)\} = \lambda [V_w][V_l]\{A_{ps}(V_i)\}, \quad i = F0, F5 \qquad (2)$$

$$\{P_{ll}(V_i)\} = \lambda [V_l]\{A_{ll}(V_i)\}, \quad i = F0, F5 \qquad (3)$$

where,

- λ = the average number of tornadoes per sq. mi. per year
- $[V_w]$ = a matrix expressing the variation of wind speed across the width of the tornado path
- $[V_l]$ = a matrix expressing the variation of wind speed along the length of the tornado path
- $A_{ps}(V_i)$ = the average area of the damage path per tornado for an F_i tornado
- $A_{ll}(V_i)$ = the average area of the life-line path per tornado for an F_i tornado.

The two average areas per occurrence of tornado are further expressed as:

$$A_{ps}(V_i) = A'(V_i) \bullet P'(V_i), \quad i = F0, F5 \qquad (4)$$

$$A_{ll}(V_i) = W_s \bullet L'(V_i) \bullet P'(V_i), \quad i = F0, F5 \qquad (5)$$

where,

- $A'(V_i)$ = the average area of the damage path for an F_i tornado obtained from the area-intensity relationship
- $P'(V_i)$ = the conditional occurrence probability of an F_i tornado given an occurrence of a tornado
- W_s = the characteristic width of a structure
- $L'(V_i)$ = the average path length of an F_i tornado.

The determination of the above six parameters, λ, $[V_w]$, $[V_l]$, $A'(V_i)$, $P'(V_i)$ and $L'(V_i)$ are summarized below.

Tornado Occurrence Rate, λ

The average occurrence rate of tornadoes in the U.S. is about 10^{-4} per square mile per year. This value can be determined either by global regionalization schemes (e.g., Refs. [7] and [8]), or by using more regional data. According to Fujita (1981), the regional occurrence rate for the BNL site is estimated as,

DISCLAIMER

Portions of this document may be illegible in electronic image products. Images are produced from the best available original document.

Table 2 Matrix, C_a, Intensity-defined Damage Area vs Reported Damage Area

	F0	F1	F2	F3	F4	F5
F0	.176	.456	.249	.098	.021	0
F1	.048	.244	.370	.266	.070	.002
F2	.013	.108	.289	.400	.175	.015
F3	.003	.030	.149	.377	.375	.066
F4	0	.011	.059	.223	.549	.158
F5	0	0	0	.098	.439	.463

Table 3 Matrix, C_l, for Path Length-Intensity Relationship (Intensity-Defined vs Reported Path Lenths)

	F0	F1	F2	F3	F4	F5
F0	.832	.099	.059	.010	0	0
F1	:563	.236	.147	.049	.005	0
F2	.379	.260	.241	.110	.010	0
F3	.156	.206	.307	.271	.060	0
F4	.039	.077	.263	.442	.140	.039
F5	0	.067	0	.666	.200	.067

$$\lambda = \frac{(40\ tornadoes)}{(30.2\ years)\ x\ (6.506 sq.mi.)} =$$

$$2.03 x 10^{-4} (tornadoes/year/sq.mi.)$$

McDonald (1982) also estimated a similar value of 2.16 x 10^{-4}. A median value of 2.1 x 10^{-4} was used for the hazard analysis of the BNL site.

Occurrence-Intensity Relationship, P(V_i)

This probability, P(V_i), represents the conditioned probability of an Fi tornado, given an occurrence of a tornado. The regional data by McDonald (1982) are directly used as tabulated below.

i	F0	F1	F2	F3	F4	F5
no.of tornadoes, N_i	11	61	31	6	1	0
$P(V_i) = N_i / \epsilon N_i$	0.100	0.555	0.282	0.055	0.009	0

The above probabilities are modified later to account for the classification errors and random encounter errors.

Area-Intensity Relationship, A(V_i)

The area-intensity relationship may be expressed in a matrix format to account for the large uncertainty in assigning a specific damage area to each tornado intensity class.

$$\{A(V_i)\} = [C_a]\{A_o(V_i)\} \qquad (6)$$

In which $A_o(V_i)$ represents a best estimate of the area of the damage path for an Fi fornado, and the site-specific values obtained by McDonald are used (1982).

i	F0	F1	F2	F3	F4	F5
$A_o(V_i)$, sq. mi.	0.0209	0.0722	0.184	0.385	0.713	1.21

The 6x6 matrix, $[C_a]$, represents the statistical relationship between the intensity-defined damage area and the reported damage area. Schaefer et al. (1980)

obtained this relationship from a statistical study of 10,204 tornadoes as given in Table 2.

Path Length-Intensity Relationship, $L(V_i)$

A similar relationship to the above Eq. (6) may be considered for the path length corresponding to an F_i tornado as,

$$\{L(V_i)\} = [C_t]\{L_o(V_i)\} \quad (7)$$

Reinhold and Ellingwood (1982) suggested the following relationship between the damage path width, and the damage path length, L:

$$W = 0.01\ L \quad (8)$$

Using this relationship, the best estimate values for the damage path length, $L_o(V_i)$, are determined as,

i	F0	F1	F2	F3	F4	F5
$L_o(V_i)$, miles	1.4	2.7	4.3	6.2	8.4	11.0

Table.3 tabulates the matrix, C_t, which was originally obtained by McDonald (1983) by analyzing 7,953 tornadoes.

Classification Errors

The foregoing three relationships, i.e., occurrence-intensity, area-intensity, and path length-intensity, are determined from observational data bases. The uncertainties associated with these determinations can be classified as direct classification errors and random encounter errors; each is represented by a 6x6 matrix, E_d and E_r, respectively.

$$\begin{aligned}\{P'(V_i)\} &= [E_r][E_d]\{P(V_i)\}\\ \{A'(V_i)\} &= [E_r][E_d]\{A(V_i)\}\\ \{L'(V_i)\} &= [E_r][E_d]\{L(V_i)\}\end{aligned} \quad (9)$$

in which, $P'(V_i)$, $A'(V_i)$ and $L'(V_i)$ are the modified relationships. Two formulations were suggested by Twisdate et al. (1981) based on the engineering judgement for the above E_d. For the random encounter errors, E_r, one suggested by Twisdale et al. (1981), and the other by Reinhold and Ellingwood (1982) are used in this study. In addition, the identify matrix is considered for both E_d and E_r to account for any possible "double counting" of the uncertainties. Overall, nine combination cases are considered for the classification errors (3 cases for E_d times 3 cases for E_r).

Variation of Wind Speed Within a Damage Path, V_w and V_t

In this hazard model, the variation of wind speed within a tornado path is considered separately along and across the path, represented by matrices, V_t and V_w in Eqs. (2) and (3). Ref. [1] describes three formulations for both V_t and V_w, which were obtained by analyzing 149 tornadoes occurring during a super outbreak in Texas on April 3 and 4, 1974. Again, nine cases are considered for modeling the variation of wind speed within a tornado path (3 cases for V_t and 3 cases for V_w).

Generation of Tornado Hazard Curves

Fig. 1 shows the generated tornado hazard curves using the above Eqs. 2, 4, 6 and 7 for the point-strike probability, which is a collection of 81 curves (9 cases of classification error formulations times 9 cases of wind-speed variation formulations). Similarly, the collection of hazard curves for a 177 ft. wide structure are generated as shown in Fig. 2, which were obtained by adding the life-line term using Eqs. 1, 3, 5, 7 and 8.

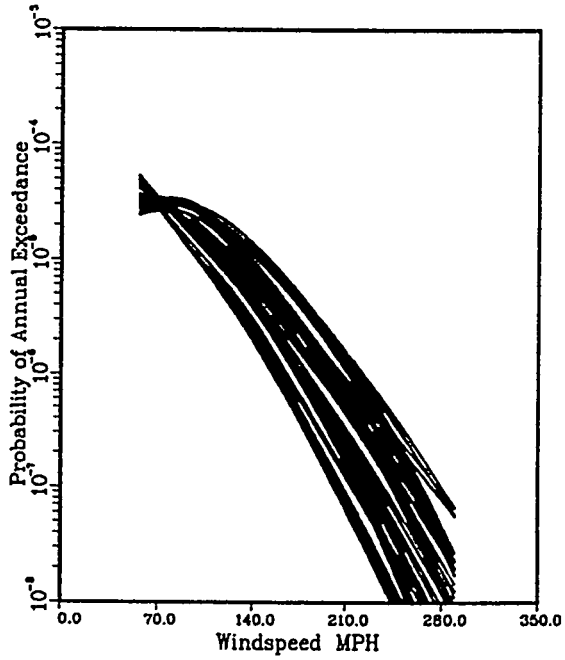

Figure 1. Generated Hazard Curves for Point Strike Risk

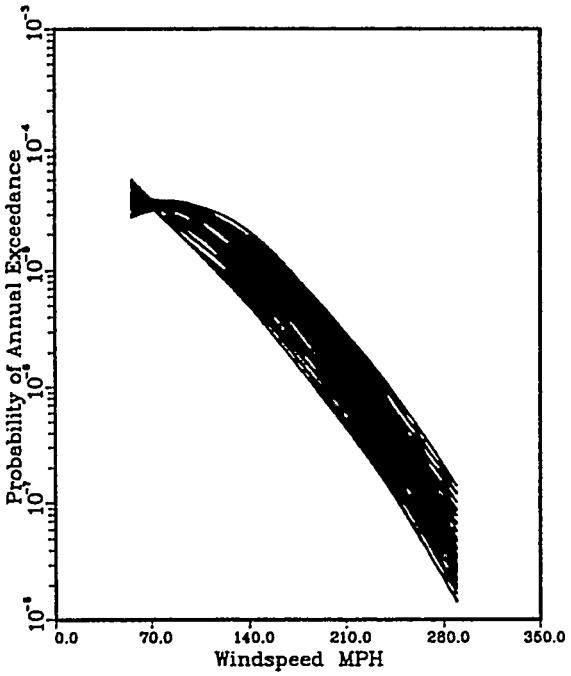

Figure 2. Generated Hazard Curves for Total Risk of 177 ft. Structure

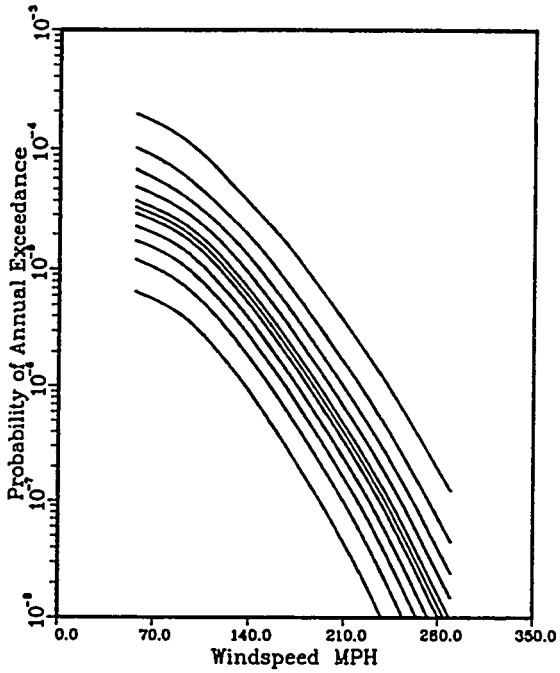

Figure 4. Tornado Hazard Curves for BNL Site (for "Point" Structures at 5, 15, 25, 35, 45, 50, 55, 65, 75, 85 and 95 Percentile)

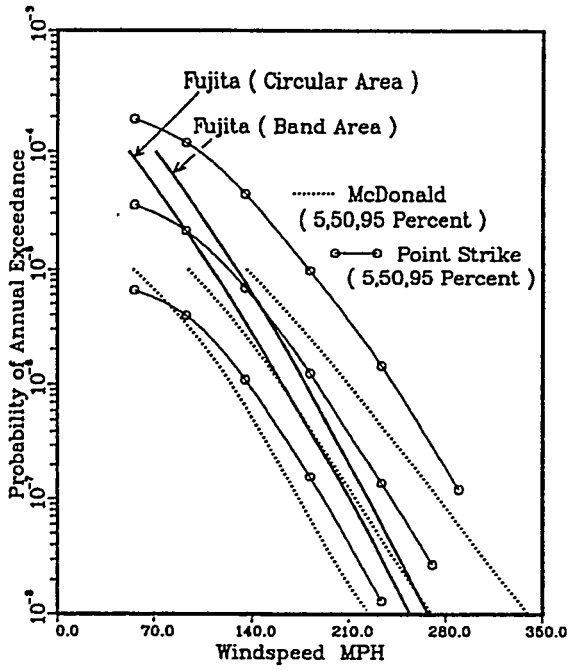

Figure 3. Comparison of Tornado Hazard Curves

The results, shown in Figs. 1 and 2, however do not account for the modeling error, i.e., the error associated with the selection and formulation of hazard model. Moreover, even using the same model may not lead to similar results due to the subjective interpretation of the formulation and the tornado data.

Fig. 3 compares the hazard curves generated for the BNL site by Fujita (1981) and McDonald (1982). Fujita generated two curves for two different definitions of the regional area surrounding the site. McDonald, on the other hand, obtained the hazard curves at 5, 50 and 95 percentile confidence levels (broken lines in Fig. 3). The best estimate curve by Fujita gives higher risk values than McDonald's median curve, although both analyses used the same data base. Based on this comparison, the additional variability of the annual probability due to modeling error was estimated to be 1.0 in terms of the lognormal standard deviation, β. By assuming the lognormal distribution for the annual exceedance probability values, p, the wind speed, V, corresponding to a confidence level in terms of the q-percentile value, is expressed as,

$$V = \exp.\left\{\beta \cdot \Phi^{-1}(q) + \ell n\, V_m\right\} \qquad (10)$$

where, β is the combined lognormal standard deviation; $\Phi^{-1}(\cdot)$ is the inverse Gaussian distribution function; and V_m is the wind speed of the median hazard curve. Fig. 4 shows the calculated point-strike hazard curves for 11 percentile values.

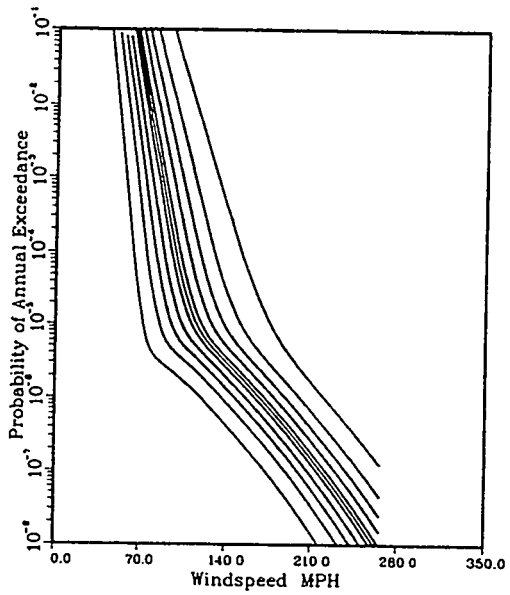

Figure 5. Combined Wind Hazard Curves at BNL Site for "Point" Structures (5, 15, 25, 35, 45, 50, 55, 65, 75, 85 and 95 Percentile)

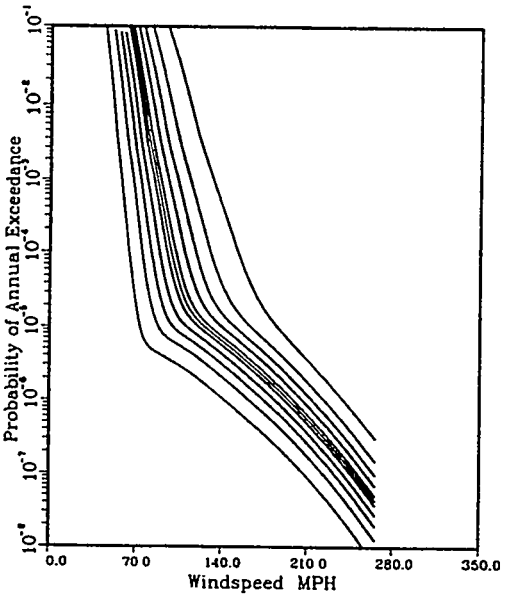

Figure 6. Combined Wind Hazard Curves at BNL Site for 177 ft. Structures (5, 15, 25, 35, 45, 50, 55, 65, 75, 85 and 95 Percentile)

COMBINED WIND HAZARD EVALUATION

According to UCRL-15910 (Ref. [3]), the following equation is recommended to convert the tornado wind speed, V_t, to the equivalent fastest-mile wind speed, V_{fm};

$$V_{fm} = 0.958\ V_t - 11.34 \qquad (11)$$

The hazard curves for straight wind were evaluated separately (Ref. [1]). The combined hazard curves were obtained using Eq. 10, and shown in Figs. 5 and 6 for the BNL site.

STRUCTURAL FRAGILITY AGAINST WIND PRESSURE

The following ASCE 7-88 formulation (Ref. [14]) is used to establish the relationship between the wind speed and the wind force, F:

$$F\ (lbs) = q\ G_n\ C_f\ A_f \qquad (12)$$

where:

q(psf)	=	$0.00256\ K\ V^2$
G_n	=	gust factor, given in Table 8 of ASCE 7-88
C_f	=	force coefficients
A_f	=	projected area normal to wind
K	=	exposure coefficient, given in Table 5 of ASCE 7-88
V	=	wind speed in mph.

The wind capacity of structures is expressed as a function of the median pressure capacity, F_m, and the random variables, ϵ_r and ϵ_u, each representing the randomness of wind forces and the uncertainty in structural capacity.

$$F_p = F_m \cdot \epsilon_r \cdot \epsilon_u$$

$$and\ \epsilon_r = \epsilon_G \cdot \epsilon_c \cdot \epsilon_d, \qquad (13)$$

$$\epsilon_u = \epsilon_s \cdot \epsilon_m$$

where:

ϵ_G	=	Factor representing variability in determining the gust factor, G_n;
ϵ_c	=	Factor representing variability in presure and force coefficients, C_f;
ϵ_d	=	Factor representing variability in wind direction;
ϵ_s	=	Factor for structural capacity; and
ϵ_m	=	Modeling error in structural analysis.

The above pressure capacity can be converted to the wind speed using the following relationship:

Table 4 Example of Fragility Evaluation of a Structure

Factor	Median Values	β_R	β_U
Basic strength	214 mph		
Structural capacity	1.0	-	0.20
Modeling	1.0	-	0.15
Gust factor	1.0	0.20	-
Pressure coefficient	1.3	0.21	-
Wind direction	1.1	0.10	-
Factors for pressure	1.43	0.31	0.25
Factors for wind speed	1.20	0.15	0.13
Total fragility	256.8 mph	0.15	0.13

$$F_v = \sqrt{F_p},\ \beta_v = 0.5\ \beta_p \qquad (14)$$

An example of the structural fragility evaluation is given in Table 4. More detailed description of the calculation procedure can be found in Ref. [1].

TORNADO MISSILE ANALYSIS

According to the USNRC Standard Review Plan [16], the total probability of missiles striking a vulnerable, critical area of the plant is estimated as a product of several probabilities. The total probability per year (P_t) is described as:

$$P_t = P_E \cdot P_{MR} \cdot P_{SC} \cdot P_p \cdot N \qquad (15)$$

where:

P_E = Probability per year of a tornado strike;
P_{MR} = Probability of missiles reaching the plant;
P_{SC} = Probability of missiles striking a vulnerable critical area of the plant;
P_p = probability of missiles exceeding the energies required to penetrate vital areas (e.g., based on wall thickness provided for tornado missiles), or producing secondary missiles which could damage vital equipment; and,
N = Number of missiles generated by the design basis event.

In this study, the 85-percentile point strike probability for F1 tornadoes, 0.637×10^{-4}, is used as a conservative estimate of the strike probability, P_E. The product of the two probabilities, $P_{MR}\ P_{SC}$, which represents an event in which a single tornado missile is picked up by a wind, and eventually hits the target structure, was estimated by a Monte-Carlo simulation. A computer program was developed for this purpose. The program generates a large number of missiles with random initial locations and random flight parameters, predicts the 3-D flight path through a time-history analysis, and perform a statistical analysis on the number of missle hits and the strike velocity. The maximum wind speed and the direction of the tornado strike also are randomized.

The probability, P_p, is determined from the kinetic energy of the missiles and the structural capacity against impact and penetration. Structural capacity is estimated from nonlinear static analysis and penetration equations. Finally, the number of potential missiles, N, is estimated by surveying the BNL site for sources of missile. Relatively weak structures, e.g., wooden buildings, utility poles, stacks, and automobiles were considered typical missile sources.

To estimate the strike probability and the velocity of a missile at impact, a set of models and assumptions are necessary, including:

- Tornado wind-field model:
- Aerodynamic charactistics of tornado missile; and
- Initial position of missile relative to the target structure and the incoming tornado.

In this study, a simple Rankine wind-field model was used to characterize the 3-D wind speed.

The trajectory and velocity of a missile are described by the following flight equations:

$$\frac{d}{dt}\overline{V_m} = \frac{1}{2}\rho\frac{C_D A}{m}\,|\,\overline{V_w} - \overline{V_m}\,|\,\left(\overline{V_w} - \overline{V_m}\right) - g\bar{z} \qquad (16)$$

in which, $\bar{V}_m$ is the missile velocity vector; V_w is the wind velocity vector; ρ is the air mass density; C_D is the drag coefficient; A is a suitably chosen area; $\bar{z}$ is the unit

Table 5 Missile Parameters

Missiles	Weight (lbs)	C_DA/m (ft^2/lb) (Best Estimate)*	(Range)
A. 6" Sch. 40 pipe (15')	285	0.0212	0.002 - 0.04
B. 12" Sch. 40 pipe (15')	740	0.016	0.002 - 0.03
C. 1" solid steel rod (3')	8	0.019	0.002 - 0.04
D. 13.5" Utility Pole (35')	1100	0.0254	0.002 - 0.05
E. Automobile	4000	0.0343	0.003 - 0.07

* From Simin and Scanlan (1978)

vector along the vertical line; m is the mass of a missile; and g is the gravitational acceleration. According to this equation, the motion of the missile depends on the flight parameter, C_DA/m and its initial condition. The following approximate formulation was suggested to estimate the flight parameter (Ref. [17]):

$$C_DA = C\left(C_{D1}A_1 + C_{D2}A_2 + C_{D3}A_3\right) \qquad (17)$$

where $C_{Di}A_i$ (i=1, 2, 3) are the values of C_DA corresponding to the principal axes of the body, and C is an empirical coefficient assumed to be 0.50 for rods, pipes and poles, and 0.33 for automobiles. Rotational movements, including a tumbling mode, are not considered in the analysis. The 4-th order Runge-Kutta method was used to numerically integrate the equations of motion.

Table 5 lists the missiles considered in the analysis. The uncertainties associated with estimating the flight parameter are considered by using random numbers, as indicated by the ranges in Table 5.

Figure 7 illustrates a simulation example in which 75 out of 1,000 tornado missiles generated from a collapsed weak wooden building hit the spherical target structure. In this simulation example, the following unknown paramters were randomized:

- Maximum tangential wind speed;
- Flight parameter of missiles; and
- Initial position of missiles (X, Y, Z corrodinates) within the building site.

In addition, the direction of the tornado path relative to the target structure (and the source of missiles) should also be randomized. Figure 8 illustrates a scheme in which the source building is represented by a "ring" that has the width, height and distance from the target building. In this scheme, the direction of the tornado path is randomized with an equal likelihood in all the directions.

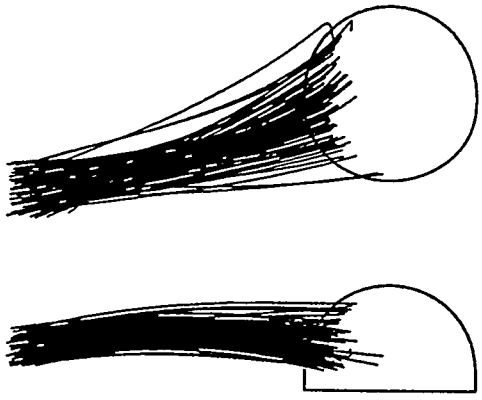

Figure 7. Trajectory of Missiles Generated due to Disintegration of a Wooden Building

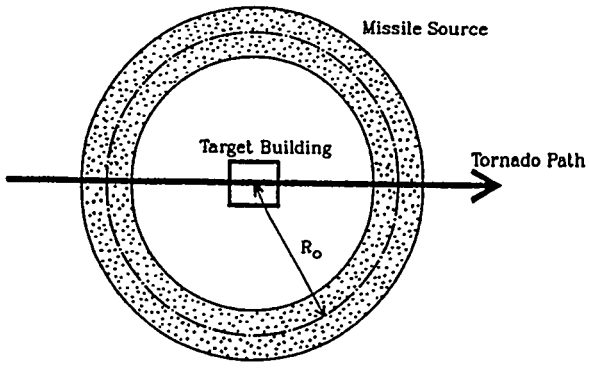

Figure 8. Circular Missile Source Surrounding the Target Building

Table 6 Number of Potential Missiles

Missile type	Distance from Target Building		
	320 ft	600 ft	1000 ft
A	400	1200	2000
B	200	600	1000
C	400	1200	2000
D	20	60	100
E	100		

Table 7 Results of Missile Simulation Analysis

Missile Type	Expected Number of Hits	Median Velocity (ft/sec.)	β of Velocity
A	22.5	118	0.15
B	8.5	97	0.12
C	22.5	118	0.15
D	1.4	119	0.14
E	3.7	96	0.18

Based on a survey of wooden structures, utility poles and parked automobiles around the target building, the number of potential missiles was estimated as listed in Table 6. The calculated strike probability drops rapidly as the distance between the initial location of the missiles and the target structure increases. The simulation results for a target building are summarized in Table 7 in terms of the number of missile hits per a tornado strike and the impact velocity.

The probability, P_p, of Eq. 15 represents the probability of missiles exceeding the kinetic energies required to penetrate the structural barrier. By assuming a lognormal distribution both for the kinetic energy of a missile, E_k, and the energy capacity of a structure against impact loads, E_s, then the probability of a missile penetration, P_p, is expressed:

$$p_p = 1 - \phi\left(\frac{ln(\overline{E_s}/\overline{E_k})}{\sqrt{\beta_k^2 + \beta_s^2}}\right) \qquad (18)$$

in which, $\overline{E}_s$ and β_s are the median and the lognormal standard deviation for the structural energy capacity; and $\overline{E}_k$ and β_k are those for missile kinetic energy.

In evaluating the structural capacity against missile penetration, empirical penetration equations (e.g., Refs. [18], [19]) can be used for small objects. However, for larger objects such as automobiles, a nonlinear structural analysis is necessary to estimate the energy absorbing capacity (Ref. [1]).

Table 8 summarizes the calculation results for a target building. To determine the effects on equipment inside the target structure, a further analysis is necessary as briefly described below.

EVALUATION OF EQUIPMENT FRAGILITY

The wind capacity of equipment housed inside a structure is determined from the following wind/tornado effects:

- Offsite power loss
- Collapse of building or part of building
- Tornado missile hit.

The fragility of equipment is expressed by the conditional probability of failure given a wind speed level expressed in terms of the fastest miles per hour (mph). However, when damage caused by tornado-borne missiles is considered, the fragility value is unconditionally defined since the variability in tornado wind speed has already been considered in the missile simulation analysis. In calculating the annual failure rate of an equipment item due to tornado missile hits, the following reduction factor should be multiplied to the probability values listed in Table 8.

Table 8 Tornado Missile Penetration Probability

Missile	Tornado Strike P_E (year $^{-1}$)	$NxP_{MR}xP_{SC}$	P_P	Penetrations per Year
A. 6 in. pipe	$0.637x10^{-4}$	22.5	1.0	$1.43x10^{-3}$
B. 12 in. pipe	$0.637x10^{-4}$	8.5	0.95	$5.14x10^{-4}$
C. 1 in. steel rod	$0.637x10^{-4}$	22.5	0	0
D. Utility pole	$0.637x10^{-4}$	1.4	0.95	$8.47x10^{-5}$
E. Automobile	$0.637x10^{-4}$	3.7	$0.3x10^{-4}$	$7.07x10^{-9}$

$$\textit{Reduction Factor} = \frac{(\textit{Area of equipment possibly hit by object})}{(\textit{Area of building possibly hit by object})}$$

An error factor (EF) of 10.0 is conservatively estimated for the annual failure rate of equipment due to tornado-borne missile hits, considering a large uncertainties involved in the tornado missile analysis as described above.

CONCLUSIONS

The methodologies for the probabilistic evaluation of a combined tornado and straight-wind hazard, and the fragility analysis of structures and equipment were described in some details.

The presented simulation scheme for the tornado-borne missiles can be used for a more rational evaluation of the plant safety.

REFERENCES

[1] Park, Y.J., "Wind/Tornado Hazard and the Fragility of Structures and Components of the HFBR," Brookhaven National Laboratory, NY, March 22, 1993.

[2] EQE Engineering Inc., "Tornado Evaluation of the ORNL High Flux Isotope Reactor," 1989.

[3] Kennedy, R.P., et al., "Design and Evaluation Guidelines for Department of Energy Facilities Subjected to Natural Phenomena Hazards," UCRL-15910, June 1990.

[4] Reed, J.W. and Ferrel, W.L., "External Wind Analysis for the Turkey Point Power Plants," NUREG/CR-4762, USNRC, March 1985.

[5] Reinhold, T.A. and Ellingwood, B., "Tornado Damage Risk Assessment," Brookhaven National Laboratory, NY, NUREG/CR-2944, September 1982.

[6] Garson, R.C., Catalan, J.M., and Cornell, C.A., Tornado Design Wind Based on Risk, Journal of the Structural Division, ASCE, Vol. 101, No. ST9, pp. 1883-1897, September 1975.

[7] ANSI N-178, "Standards for Estimating Tornado, Hurricane and Other Extreme Wind Parameters at Nuclear Power Site," American National Standard Institute, New York, June 1979.

[8] Markee, E.H., et al., "Technical Basis for Interim Regional Tornado Criteria," WASH-1300, U.S. Governement Printing Office, Washington, May 1974.

[9] Fujita, T.T., "Tornado and High-Wind Hazards at Brookhaven National Laboratory Site, New York," report prepared for Lawrence Livermore National Laboratory, Livermore, CA, 1981.

[10] McDonald, J.R., "Assessment of Tornado and Straight Wind Hazard Probabilities at the Brookhaven National Laboratory, Long Island, New York," report prepared for Lawrence Livermore National Laboratory, Livermore, CA, October 1982.

[11] Schaefer, J.T., et al., "Tornado Track Characteristics and Hazard Probabilities," Proceedings of the Fifth International Conference on Wind Engineering," Pergamon Press, New York, pp. 95-109, 1980.

[12] McDonald, J.R., "A Methodology for Tornado Hazard Probability Assessment," Institute for Disaster Research, Texas Tech. University, NUREG/CR-3058, October 1983.

[13] Twisdale, L.A. and Dunn, W.L., " Tornado Missile Simulation and Design Methodology, Vols. 1 and 2," EPRI Report NP-2005, EPRI, Palo Alto, CA, August 1981.

[14] ASCE, "Minimum Design Loads for Building and Other Structures," ANSI/ASCE 7-88, Nov. 27, 1990.

[15] Mehta, K.C., "Wind Speed Estimates: Engineering Analysis," Proceeding on the Symposium on Tornadoes, Texas Tech. Univ., Lubbock, TX, pp. 89-103, June 1976.

[16] USNRC, "Standard Review Plan, NUREG-0800," July 1981.

[17] Simin, E. And Scanlon, R.H., Wind Effects on Structures, John Wiley & Sons, New York, NY, 1977.

[18] Gwaltney, R.C., "Missile Generation and Protection in Light-Water Cooled Power Reactor Plants," ORNL, NSIC-22, Oak Ridge National Laboratory, Oak Ridge, TN, 1968.

[19] Russell, C.R., Reactor Safeguards, MacMillan, NY, 1962.

DISCLAIMER